Received: 24 April 2026, Revised: 23 May 2026, Accepted: 08 June 2026, Online: 17 June 2026

DOI: https://dx.doi.org/10.55708/js0506003

Superconductivity Research Method Based on Atomic Properties and Hole-Electron Tensor

Guohua Zhang [*1,2], **Xiyu Zhang** [3]

[1] Shenzhen Polytechnic University, Shenzhen, 518000, China

[2] R&D Department Shenzhen Hengdrive Technologies Co. Ltd, Shenzhen, 518100, China

[3] Israel Institute of Technology Guangdong, Shantou, 515000, China

Email(s): Hansun.zhang@hengdrive.com (Guohua zhang), zhang52016@gtiit.edu.cn (xiyu zhang)

*Corresponding author: Guohua Zhang, Shanhai Shangcheng, Tongda Road, Xixiang, Baoan, Shenzhen, Guangdong, 518103, China. Email: 617620347@qq.com

ABSTRACT: The microscopic mechanism of superconducting critical temperature (Tc) remains a long-standing unsolved problem in condensed matter physics. Based on de Broglie's matter wave theory, this work introduces the concepts of superconducting gene (SCG) and superconducting DNA (SCD). A phenomenological model is proposed that relates Tc to the number of orbital electron-hole pairs (N), the mass of SCD, and the diameter of SCG. The model is validated across multiple material families, including copper oxides, iron-based superconductors, and high-pressure hydrides.

It is found that the critical temperature of superconductivity can be effectively increased by adjusting the electron orbital filling (N), SCG (a), and introducing light element heterojunctions. Based on this, the "orbital engineering" strategy is proposed, which provides a new path to break through the bottleneck of room-temperature superconductivity. In addition, isotope effect of all superconductors is verified by the general superconducting formula, which further guides the design of effective components of high-temperature superconductors.

This work attempts to incorporate the isotope effect of BCS theory superconductor and strong correlation theory superconductor into a unified phenomenological framework, providing a consistent description of the critical temperature mechanism across different types of superconductors.

A hole-electron model based on electron and hole arrangement is constructed, which can dynamically describe the formation, division and recombination processes of carrier pairs, so as to more accurately simulate the superconductivity mechanism.

This study not only makes important theoretical progress, but also provides a solid foundation and innovative ideas for future design and development of new superconducting materials. By combining pressure/doping regulation, light element heterojunction design and other methods, it is expected to achieve superconducting materials with higher critical temperatures and promote the application and development of superconducting technology.

KEYWORDS: Superconduct, BCS, Isotope effect

1. Introduction: The century-old evolution and unsolved mysteries of SC theory

Since the discovery of superconductivity in mercury in 1911 [1], superconductivity research has progressed through three major milestones.

The BCS theory [2], proposed in 1957, successfully explains conventional superconductors such as Nb_3Sn (Tc ~ 18 K) based on Cooper pair formation via electron-phonon coupling, but predicts a theoretical limit of Tc ≤ 40 K [2].

The discovery of high-temperature superconductivity in the La-Ba-Cu-O system in 1986 [3] revolutionized the field, challenging the BCS paradigm and leading to the development of new theoretical frameworks including strong correlation theory and resonant valence bonding.

More recently, the discovery of superconductivity in H_2S at 200 K under 150 GPa [4] opened a new dimension of high-pressure superconductivity research.

However, the existing theories still face three major challenges:

- For copper oxides, the competition between pseudogap, striped phase, and superconducting state in doping phase diagrams remains unresolved [5];
- For iron-based superconductors, the symmetry of multi-orbital magnetic fluctuations and the nature of superconducting order parameters are still under debate [6];
- For room-temperature superconductivity, the stability and mechanism of carbonaceous sulfur hydrides (e.g., C-S-H, Tc ~ 287 K [7]) remain controversial.

In addition to these experimental challenges, existing theoretical approaches also have significant limitations. Eliashberg theory, while successful for conventional superconductors, becomes computationally intractable for strongly correlated systems [8]. Strong correlation models based on the Hubbard Hamiltonian can capture many features of cuprate superconductivity but lack predictive power for Tc [9]. Recent machine learning approaches have shown promise for Tc prediction but provide limited physical insight [10].

This paper aims to construct a bridge and quantitatively correlate microscopic electronic structures with macroscopic TC, providing a new paradigm for room-temperature superconducting design.

2. Theoretical Part

2.1. BCS theory and its extension

At the heart of the BCS theory lies the cooperative cohesion induced by electron-phonon coupling, which has a Tc formula of:

$$T_c = 1.13\omega_D \exp\left(-\frac{1}{N(E_F)V}\right) \quad (1)$$

here ωD : the Debye freq; N(EF) : the Fermi plane density; V : the attraction potential.

- Successful case: Double-band superconductivity of MgB_2 (Tc=39K [11]) can be accurately described by the Eliashberg equation [8];
- Limitations: It cannot explain the d-wave pairing and pseudo-bandgap phenomena in copper oxides [9].

2.2. Strong correlation with the Hubbard model

For copper oxides, Mott physics and Hubbard models have become mainstream:

- T-J model: hole doping leads to spin singlet resonances in antiferromagnetic background [10];
- Pseudogap origin: preformed Cooper pair vs topological order parameter [12].
- Controversy: ARPES displays Fermi arcs instead of closed surfaces [13], challenging traditional paired images.

2.3. Quantum critical fluctuation mechanism

In iron-based superconductors, spin fluctuations near the antiferromagnetic quantum critical point mediate *s*±-wave pairing [14], but cannot explain pressure-induced *non-monotonic changes in Tc* [15].

2.4. Revival of high-pressure hydride and electron-phonon coupling

The ultra-high Tc of H2S and LaH_{10} re-highlights the importance of electron-phonon coupling [16], but first-principles calculations show that:

- High-frequency phonons (H-H bond vibration) dominate the coupling strength [17];
- Electron associations in metal hydrides cannot be ignored [18].

2.5. Acoustic excitons excitation model

Phonon can be treated as matter wave, the energy of the acoustic exciton is expressed as $\varepsilon_k = \hbar_k v_0$ ($v_0 = v_1$), v_1 is the frequency of the carrier. This model is a thermal excitation model of monotonic excitons, which is called the mono excitation model [19]. Image:



Figure 1. Acoustic excitons excitation model

2.6. No dissipative conductivity mechanism

Before and after the acoustic excitation process, the crystal lattice and carriers do not change in any way, but there are acoustic excitons in the middle that participate in the conductive process of the carriers. (Figure below)

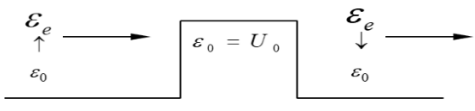


Figure 2. Non-dissipative conductive mechanism [19]

In this state, the conductor will not consume energy to complete the conductive process. In this proposed

mechanism, conduction occurs without net energy dissipation because the energy absorbed from phonons during carrier acceleration is exactly balanced by the energy released during deceleration.

When acoustic excitons participate in conduction as intermediate states, the energy of the initial and final state grids and carriers is conserved, and the phonon absorption and emission process cancel out, and the total energy remains unchanged. Electrons achieve directional motion by periodically exchanging acoustic excitons without overcoming lattice scattering, so the resistance is zero.

2.6.1. *The band structure of electrons in a one-dimensional periodic potential*

Generally, the conductor of the solid phase is composed of crystals. The movement of carriers in crystals can be simplified to move in 1D periodic field. The 1D periodic field U(x) as shown in the figure consists of a square barrier.

$$U(x) = U(x + n_0 a) \tag{2}$$

here n_0 is an integer; a is the lattice dimension of the 1D lattice; a=c+b; and U(x) is periodic [19].

$$U(x) = \begin{cases} 0 & (n_0 a \le x \le n_0 a + c) \\ U_0 & (n_0 a - b < x < n_0 a) \end{cases} \tag{3}$$

The image is:

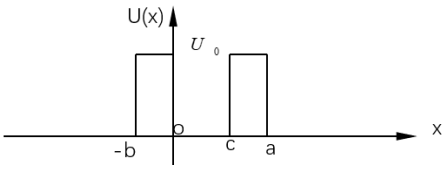


Figure 3. One-dimensional periodic square potential trap [19]

According to the Kronig-Penner model, the electron wavefunction satisfies Bloch's theorem ψ(x+a)=eikaψ(x), and solves the Schrödinger equation in sections.

The wavefunctions in the potential well region (0<x<b) and the barrier region (b<x<a) are:

$$\psi_I = Ae^{iqx} + Be^{-iqx} \tag{4}$$

$$\psi_{II} = Ce^{ikx} + De^{-ikx} \tag{5}$$

where q=(2mE)^0.5/ħ, κ=(2m(U0−E))^0.5/ħ. Through the wave function continuity condition and the Bloch condition, the band equation is obtained

$$\cos(ka) = \cos(qb)\cosh(kc) + \frac{k^2+q^2}{2qk}\sin(qb)\sinh(kc) \tag{6}$$

This equation determines the band structure of the electron energy E(k).

2.6.2. *Acoustic exciton formation conditions*

When the natural frequency ω c of the carrier (electron) matches the phonon frequency ω, the resonance absorbs/emits phonons to form acoustic excitons. The natural frequency of electrons has the relationship with the energy band dispersion as below:

$$\omega_c = \hbar k/(m^* a) \tag{7}$$

where m∗ is the effective mass of the electron. When ωc=ω, phonon wave vector q=1/a (near the Brillouin zone boundary), the change in electron momentum satisfies Δk=q, and the energy conservation condition is:

$$E(k+q) = \hbar\omega \tag{8}$$

At this time, electrons and phonons are strongly coupled to form acoustic excitons, and their energies are:

$$E_s(\omega_c) = \hbar^2 k^2/(2m^*) + \hbar\omega \quad (when \ \ \omega_c = \omega) \tag{9}$$

2.7. *Modeling and derivation of critical temperature superconductivity formula*

2.7.1. *Derivation of the General Superconducting Critical Temperature Formula*

Only electrons within a range of $k_B T$ around the Fermi level can be excited, meaning only a fraction of electrons proportional to $k_B T/E_F$ are affected. Consequently, the number of excited electrons is approximately the $n(k_B T/E_F)$, and each excited electron absorbs an energy of $k_B T$. On average, the total thermal kinetic energy is approximated as [20].

$$E_e = \frac{n(k_B T)^2}{E_F} \tag{10}$$

More precise structure the total thermal kinetic energy of finer structure is accurately calculated as:

$$E_e = \frac{n(\pi k_B T)^2}{6E_F} \tag{11}$$

So the heat capacity is:

$$C_e = \frac{\partial E_e}{\partial T} = \frac{\pi^2 n {k_B}^2 T}{3E_F} = \pi^2 R\frac{k_B T}{3E_F} = \gamma \mathrm{T} \tag{12}$$

Ce : the specific heat of electrons; T: temperature;

γ: the specific heat coefficient of electrons [21];

$R = nk_B$;

In SC, phonon can be treated as De Broglie's Matter Wave, and the stable state depends on satisfying the condition of phase wave resonance as $\lambda = Na$, $\mu = Nm$.

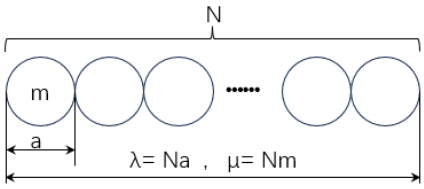


Figure 4: De Broglie's material wave model of superconductivity theory

By De Broglie's Matter Wave Formula:

$$\mathrm{p} = \frac{h}{\lambda_\mathrm{p}} \tag{13}$$

Phonon wave length $\lambda_\mathrm{p} = \lambda = \mathrm{N} * \mathrm{a}$, that is, the wave length of SC, is an integral multiple of a (the length of the lattice constant).

The "effective mass" (m_p) of phonons is used to describe the behavior of phonons as they propagate in solids. It is has the relationship of phonons dispersion as following:

$$m_p = \frac{\hbar^2}{(\frac{\mathrm{d}^2 E_p}{\mathrm{d}k_{wv}^2})} \tag{14}$$

ħ: the reduced Planck constant;

E_p : the phonon energy;

k_{wv}: the wave-vector; $(\frac{\mathrm{d}^2 E_p}{\mathrm{d}k_{wv}^2})$ is the 2nd derivative relative to the wave-vector. $k_{wv} = {}^{2\pi}/_{\lambda_\mathrm{p}}$ [22] where is the λ_p phonon wavelength and π is pi. Solution:

$$E_p = \frac{4\pi^2\hbar^2}{m_p{\lambda_\mathrm{p}}^2} = \frac{\mathrm{h}^2}{m_p{\lambda_\mathrm{p}}^2} \tag{15}$$

$\mathrm{m_p}, \lambda_\mathrm{p}$ is a physical quantity related to a and m in the crystal lattice [19]. $\mathrm{m_p}$ is the "effective mass" of phonons, a physical quantity used to describe the behavior of phonons as they propagate in solids, associated with lattice m. $\mathrm{m_p} = \mathrm{k_{mp}} * \mathrm{N} * \mathrm{m}$; $\mathrm{k_{mp}}$ is a constant between phonons and crystal lattices; $\mathrm{m} = \sum m_i$, m_i is the atomic weight of the SCD atoms in the superconducting lattice; $\mathrm{a} = \sum a_j$, a_j is the atomic diameter of the SCG atoms in the superconducting lattice (see Appendix: Periodic Table of Atomic Radius). h is Planck's constant, $\mathrm{E_p}$ is the energy of the phonon. We can get:

$$\mathrm{E_p} = \frac{\mathrm{h}^2}{\mathrm{m_p}*{\lambda_\mathrm{p}}^2} = \frac{\mathrm{h}^2}{\mathrm{k_{mp}}*\mathrm{N}*\mathrm{m}*\mathrm{N}^2*\mathrm{a}^2} = \frac{\mathrm{h}^2}{\mathrm{k_{mp}}*\mathrm{m}*\mathrm{a}^2*\mathrm{N}^3} \tag{16}$$

Equation (16) shows that the phonon energy is inversely squared to the coherence wavelength.

According to the previous definition of acoustic excitons, when the natural frequency ω_c of the carrier (electron) is the same as the phonon frequency ω, the electron absorbs the energy of the phonon and the acoustic exciton is generated. The superconducting mechanism begins. At this time, the specific heat of superconducting electrons is

$$\mathrm{C_s} = \frac{\mathrm{dE_s}}{\mathrm{dT}} = \frac{\mathrm{d(E_e + E_p)}}{\mathrm{dT}} = \frac{\mathrm{dE_e}}{\mathrm{dT}} + \frac{\mathrm{dE_p}}{\mathrm{dT}} = \gamma\mathrm{T} + \frac{\mathrm{dE_p}}{\mathrm{dT}} \tag{17}$$

It explains that when electrons are at the critical temperature of superconductivity, the specific heat of electrons suddenly becomes larger.

At the same time, because of $\mathrm{E_p}$=$\mathrm{E_e}$, we get:

$$E_p = \frac{\mathrm{h}^2}{\mathrm{k_{mp}}*\mathrm{m}*\mathrm{a}^2*\mathrm{N}^3} = E_e = \frac{n(\pi k_B T_c)^2}{6E_F} \tag{18}$$

$$\frac{\mathrm{h}^2}{\mathrm{k_{mp}}*\mathrm{m}*\mathrm{a}^2*\mathrm{N}^3} = \frac{n(\pi k_B T_c)^2}{6E_F} \tag{19}$$

Left side is the energy of the electron in Tc, right side is the energy of the acoustic exciton. When both sides are equal, the temp is the superconducting critical temperature of the superconductor. Rearranging equation (18) gives:

$$T_c = \sqrt{\frac{6E_F h^2}{n*\pi^2*{k_B}^2*\mathrm{k_{mp}}*\mathrm{N}*\mathrm{m}*\mathrm{N}^2*\mathrm{a}^2}} = \frac{K_T}{\sqrt{N^3 m a^2}} \tag{20}$$

We have made this formula a general superconducting formula for the critical temperature of superconductors [19]. This formula applies to all superconductors, including low-temperature superconductors, high-temperature superconductors, ambient temperature superconductors, oxide superconductors, and hydride superconductors. In this formula, m is the summary of the atom mass of superconducting DNA, the unit is u, and a is the sum of all atomic diameters of the superconducting gene, in angrims (Å); N is a positive integer; where the universal constant K_T is defined as:

$$K_T = \sqrt{\frac{6E_F*h^2}{n*\pi^2*{k_B}^2*\mathrm{k_{mp}}}} = \frac{h}{k_B}\sqrt{\frac{6E_F}{n*\pi^2*\mathrm{k_{mp}}}} \tag{21}$$

E_F is the unit of eV,

h the unit of is J*s,

k_B the unit of is $J * Kelvin^{-1}$,

n and $\mathrm{k_{mp}}$ is the dimensionless number,

the K_T unit of is $Kelvin * Å * u^{0.5}$,

u is atomic weight.

Then the unit converted of $K_T/\sqrt{N^3 m a^2}$ is Kelvin.

Below is the process of calculating K_T .

$h = 6.6261 * 10^{-34}\ J * s$;

$k_B = 1.3806 * 10^{-23}\ \frac{J}{\mathrm{Kelvin}}$; $\pi = 3.14159$;

Suppose: $E_F = 5\ eV = 8.0109 * 10^{-19} J$; For all the superconductors, the effective electron-phonon coupling number of Fermi surfaces: $n * \mathrm{k_{mp}} = 1$;

$$\frac{h}{k_B} = \frac{6.626*10^{-34}}{1.3806*10^{-23}} = 4.7992 * 10^{-11} K * s \ ;$$

$$\pi^2 * n * \mathrm{k_{mp}} = 9.8696 \ ;$$

$$\sqrt{\frac{6E_F}{\pi^2 * n * \mathrm{k_{mp}}}} = \sqrt{\frac{6*8.0109*10^{-19}}{9.8696}} = 6.9785 * 10^{-10} \ \ J^{0.5} \ ;$$

$$K_T = \frac{h}{k_B}\sqrt{\frac{6E_F}{\pi^2 * \mathrm{n} * \mathrm{k_{mp}}}}$$
$$= 4.7992 * 10^{-11} * 6.9785 * 10^{-10}$$
$$= 3.3480 * 10^{-20}\ K * s * J^{0.5}$$
$$= 3.3480 * 10^{-20}\ K * kg^{0.5} * m$$

Due to:

$$1\ J^{0.5} = 1\ kg^{0.5} * m/s;$$

$$1\ kg^{0.5} * m = \sqrt{1.6605 * 10^{27}\ u} * 10^{10} \text{Å};$$

$$= 7.7602 * 10^{23} u^{0.5} * \text{Å} \ ;$$

After calculation, it can be obtained:

$$K_T = 3.3480 * 10^{-20} * 7.7602 * 10^{23}$$

$$= 25981\ \ K * u^{0.5} * \text{Å} \ ;$$

The fitted value of the universal constant $K_{T-exp} = 25434\ K * \text{Å} * u^{0.5}$, which is derived from experimental data across the 22 different superconducting families in table 2 [19]. Only 2.15% difference between theoretical and experimental values.

2.7.2. *Significance of the general superconductivity formula*

We can derive from the general superconductivity formula $T_c = \frac{K_T}{\sqrt{N^3 m a^2}}$ from (20):

1) The index of the isotopic effect is automatically given as -0.5: the sum of the Tc and the atomic weight of the superconducting DNA satisfy the inverse square root relationship. The isotopic effect predicted by BCS theory α=-0.5 is only applicable to conventional metal superconductors. For copper oxides and iron-based superconductors, the isotopic effects measured by experiments deviate significantly from this value, which has become a long-term problem in superconductivity research. The general formula naturally contains the √m factor, so it automatically gives an isotopic effect of α= -0.5. This means that regardless of whether the pairing mechanism is electron-phonon coupling (BCS) or spin fluctuation (strong correlation), as long as the formula is met, it will be uniformly represented as α= -0.5. This is the first time that the isotopic effects of BCS theory superconductor and strong association theory superconductor are included in a unified framework.

For example, when replacing CuO in the plane, according to the available data,$O^{18}O^{16}$ Tc is proportional to the power of -0.1 of the mass ratio, i.e. $T_c \propto M^{-\alpha} = M^{-0.1}$ [23].

The calculation obtains: $\frac{T_c(O^{16})}{T_{c1}(O^{18})} = \left(\frac{16}{18}\right)^{-0.1} = 1.012$

According to the general superconductivity formula, the mass of DNA is m(CuO^{18})=81.6 u and m(CuO^{16})=79.6 u;

$$\frac{T_c(CuO^{16})}{T_{c1}(CuO^{18})} = \frac{\sqrt{m_1}}{\sqrt{m}} = \frac{\sqrt{CuO^{18}}}{\sqrt{CuO^{16}}} = \frac{\sqrt{81.6}}{\sqrt{79.6}} = 1.012 \qquad (22)$$

The theoretical results are completely consistent with the results of the measurements, which proves the correctness of the theory. For all superconductors, the isotopic effect index of their superconducting DNA is -0.5.

Based on isotopic effects, the superconducting DNA and superconducting genes of superconductors can be calculated. For the 20 material in table 2, the alpha of SCD mass is -0.5.

Through isotopic effects, we can determine their index and thus determine the superconducting DNA and superconducting genes of high-temperature superconductors. In addition, combined with the structural properties and isotopic effect of high-temperature superconductors, we can take crystal design or elemental substitution (element displacement) to increase the critical temperature of superconductor.

2) It is derived that high-pressure strength induction is another effective means to add the critical temperature of superconductors, which increases Tc by compressing lattice parameter a. The partial derivation of the pressure P for the critical temperature superconductivity formula:

$$\frac{\partial T_c}{\partial P} = \partial\left(\frac{K_T}{\sqrt{N^3 m a^2}}\right)/\partial P$$

$$= -\frac{1}{a}\frac{K_T}{\sqrt{N^3 a^2 m}}\frac{\partial a}{\partial P} - \frac{1}{2m}\frac{K_T}{\sqrt{N^3 a^2 m}}\frac{\partial m}{\partial P} - \frac{3}{2N}\frac{K_T}{\sqrt{N^3 a^2 m}}\frac{\partial N}{\partial P}$$

Translates to:

$$\frac{\partial T_c}{T_c \partial P} = -\frac{\partial a}{a \partial P} - \frac{1}{2}\frac{\partial m}{m \partial P} - \frac{3}{2}\frac{\partial N}{N \partial P} \qquad (23)$$

$$\frac{\partial \ln(T_c)}{\partial P} = -\frac{\partial ln(a)}{\partial P} - \frac{1}{2}\frac{\partial ln(m)}{\partial P} - \frac{3}{2}\frac{\partial ln(N)}{\partial P} \qquad (24)$$

For H_2S, a is long a=1.66 Å, N=10, at atmospheric pressure $T_c = 40K$. At 150 GPa, a becomes short, a=1.34Å,

N=3, and the compression lattice constant a↓23% → superconducting critical temperature Tc↑160 K.

3) The elemental hybrid research method of high-temperature superconductors has been proven to be effective. The lattice size may change very little after mixing. However, it will cause the ionization energy to change, and the ionization energy will affect the number of N. According to function (16), N may greatly affect the critical temperature value.

2.8. Research methods of hole-electron tensor model

Considering the acoustic exciton, the Schrödinger equation can be written as:

$$[-\frac{h^2}{2m}\sum_{i=1}^{M}\nabla_i^2+\sum_{i=1}^{M}V(r_i)+\sum_{i=1}^{M}\sum_{j<i}\mathrm{U}(r_i,r_j)+\sum_{i,k}^{N_1}\sum_{j,l}^{N_2}\mathrm{W}(r_{i,j},r_{k,l})]\psi=\mathrm{E}\psi \quad (25)$$

where is an integer, the four terms in square brackets are i,j,k,l,M,N_1,N_2 the kinetic energy of each electron, the energy between each electron and all nuclei, the energy between different electrons, and the energy between electrons and phonons. When the temperature is above the critical temperature, $\sum_{i,k}^{N_1}\sum_{j,l}^{N_2}\mathrm{W}(r_{i,j},r_{k,l})$ this part of the action energy is close to zero. However, when the temperature is close to the critical temperature, the role of this part can not be ignored.

$$\sum_{i,k}^{N_1}\sum_{j,l}^{N_2}\mathrm{W}(r_{i,j},r_{k,l})=\sum_{i,k}^{N_1}\sum_{j,l}^{N_2}J_{i,j,k,l}s_{i,j}s_{k,l}+\sum_{i,j}^{N_1}h_{i,j}s_{i,j} \quad (26)$$

$J_{i,j,k,l}$ is the coupling coefficient, $h_{i,j}$ is the external magnetic field, when the $N_1=N_1$, tensor is a two-dimensional square array, the phenomenon of superconductivity will occur at this time, and the relationship between the temperature and the magnetic field of the superconductor can be deduced with this formula. Simplify this formula

$$W=\sum_{<i,j>}^{N}J_{ij}s_is_j+\sum_i^N h_is_i \quad (27)$$

This formula is the form of the Sherington-Kirkpatrick model [24]. where the coupling coefficient:

$$J_{NN}=\begin{bmatrix}J_{11} & \cdots & \cdots & \cdots & J_{N1}\\ \cdots & J_{22} & \cdots & \cdots & \cdots\\ \cdots & \cdots & \cdots & \cdots & \cdots\\ \cdots & \cdots & \cdots & \cdots & \cdots\\ J_{1N} & \cdots & \cdots & \cdots & J_{NN}\end{bmatrix} \quad (28)$$

N_1 represents the No. of electron holes (HE) in the superconducting gene,

N_1 = ∑No. of electrons + ∑No. of electrons or holes requested for filling track = ∑e + ∑H (29)

N_2 represents the No. of genes in the superconducting unit cell, which is N in the general superconducting formula.

The hole-electron tensor model is a tensor model composed of N_1 and N_2, and when $N_1 = N_2$, the phonon becomes an acoustic exciton.

The tensor composed of all electrons and holes is the least energy required to form a carrier only when the No. of rows and columns is the same and the diagonal is all electrons (the rest are electrons or holes), and the energy required for electrons and electrons, or when electrons and holes form carriers, is the least and most stable. Electrons and electrons, or sometimes electrons and holes form carriers, move the transmitted current and then split into electrons and holes, and then form new carriers with new electrons or holes. Such carriers continue to combine, transmit current, split, and then recombine, and repeat to form a superconducting mechanism.

The construction of this hole-electron tensor composed of electrons and holes: the No. of rows is the sum of the No. of electrons and holes in the superconducting gene, and the No. of columns is the No. of unit cells. The No. of rows is equal to the No. of columns.

$$\begin{bmatrix}e & \cdots & \cdots & \cdots & \cdots\\ \cdots & e & \cdots & \cdots & \cdots\\ \cdots & \cdots & \cdots & \cdots & \cdots\\ \cdots & \cdots & \cdots & e & \cdots\\ \cdots & \cdots & \cdots & \cdots & e\end{bmatrix} \quad (30)$$

In this tensor, the diagonal is electron, and the rest of the positions can be electrons or holes.

2.8.1. Decomposition of tensor structure

For hole-electron tensor models:

$$\mathcal{H}=\sum_{ij}^{N_1}\sum_{kl}^{N_2}J_{i,j,k,l}e_i^{\dagger}e_jH_k^{\dagger}H_l \quad (N_1=N_2=N) \quad (31)$$

Physical meaning of operators:

- $e_i^{\dagger}e_j$: the transition of electrons in orbit $i \rightarrow j$;
- $H_k^{\dagger}H_l$: the transition of holes in orbit $k \rightarrow l$;
- N_1, N_2 : the degeneracy of the track; N is the No. of SCGs;
- $J_{i,j,k,l}$: Coupling coefficient.

Diagonal cell: at that time, there is $i=j \ \ and \ \ k=l$

$$\mathcal{H}_{diag}=\sum_i^{N_1}\sum_k^{N_2}J_{i,k}e_i^{\dagger}e_iH_k^{\dagger}H_k \quad (32)$$

At this point, both electrons and holes remain constant in their respective orbits, and the diagonal element is actually the density-density interaction of electrons and holes.

2.8.2. Diagonal superconductivity criterion

When the diagonal element is in the electronic state (), the system reaches the minimum excitation state energy:$i = j \ \ and \ \ k = l \ \ and \ \ N_1 = N_2 = N$;

$$\Delta E_{min} = \min\{\langle ij|\mathcal{H}|kl\rangle\} = \min\{\langle i|\mathcal{H}_{diag}|k\rangle\}$$
$$= \min\{\langle N|\mathcal{H}_{diag}|N\rangle\} \quad (33)$$

The corresponding density matrix

$$\rho_{HE} = \sum_{m=1}^{N_1} |\Psi_m\rangle \langle\Psi_m| \quad (34)$$

- Electron-hole entanglement state:
- $|\Psi_m\rangle = \frac{1}{\sqrt{2}}\left(e_{q\uparrow}^{\dagger}H_{k\downarrow}^{\dagger} + e^{i\phi}e_{q\downarrow}^{\dagger}H_{k\uparrow}^{\dagger}\right)|0\rangle$
- N_1:Orbital degeneracy ($N_1 = N$)
- $e_{q\uparrow}^{\dagger}$: momentum q is the operator produced by the electron of the spin ↑; $H_{k\downarrow}^{\dagger}$: momentum k is the operator produced by the hole of the spin ↓.
- $e_{q\uparrow}^{\dagger}H_{k\downarrow}^{\dagger}$ The electrons ↑of the spin are paired with the holes of the spin; ↓ $e^{i\phi}e_{q\downarrow}^{\dagger}H_{k\uparrow}^{\dagger}$ The electrons of the phase-modulated spin ↓ are paired with the holes of the spin ↑;
- ϕ: Quantum phase, when $\phi = 0$, s-wave pairing, when $\phi = \pi$, d- wave pairing.

In this tensor structure, electrons and electrons, electrons and holes can form carrier pairs well and effectively, and these carrier pairs are not fixed, but these carrier pairs are constantly split and combined to achieve the effect of superconductivity. Dynamic carrier pairs form the basis of superconductivity.

1) After electrons and electrons, electrons and holes form carriers, they are associated with lattice vibrations, rather than cooper pairs.
2) Electrons and electrons, electrons and holes are constantly combined to form carriers (phonons that absorb lattice vibrations), and then continue to split (release phonons to the crystal lattice), and then form new carriers with new electrons or holes.
3) In this hole-electron tensor model, the carrier's trajectory is along the electron.
4) In this hole-electron tensor model, if only the diagonal has electrons, and the other positions are holes, then the carrier's path of motion is the shortest. The shortest path is the highest energy obtained by the carrier, corresponding to a high critical temperature of the superconductor. If the diagonal is electrons, and there are electrons elsewhere, then the carrier's path of motion becomes longer, corresponding to a lower critical temperature. If there is a hole in the diagonal, that is, N_1 is not equal to N_2, a superconductor will not form.

In this theory, superconductivity can be achieved by no longer requiring electron pair stability as in BCS theory. Therefore, it can explain the formation mechanism of high-temperature superconductivity.

The only requirement is to form a resonance according to the De Broglie matter wave, that is, the sum of the No. of electrons + the No. of holes is equal to the No. of superconducting unit cells.

For better description, the part that determines the size of a and the value of N_1 is called the superconducting gene, or SCG for short. The part that determines the m size is called superconducting DNA, or SCD for short. An SCD contains an SCG. N SCDs form superconducting unit cells, referred to as SCCs.

From this hole-electron tensor model, we can conclude that;

1) All-metal superconductors such as Hg, Al, Pb, and Sn have a low superconducting critical temperature because the hole-electron tensor is full of electrons and has a long motion path.
2) In the superconducting gene, the elements that contribute electrons are in the light elements in the first, third and eleventh columns of the periodic table, that is, the light elements in the s^1 and d^1 orbitals, and the elements that form holes in the light elements in the sixteenth column of the periodic table have a higher critical temperature of the superconductors.
3) It is predicted that the light elements in the s^1 and d^1 orbitals and the light elements in columns 17 and 18 of the periodic table should have high critical superconducting temperatures. The superconductor of the s^1 orbital is more stable than the superconductor of the d^1 orbital.

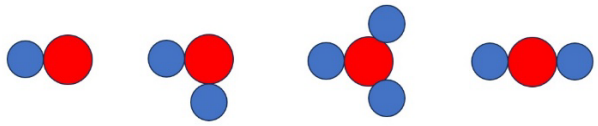
For example, the hole-electron tensor structure of the superconducting gene CuO is as follows:

$$\begin{bmatrix} e & H & H \\ H & e & H \\ H & H & e \end{bmatrix} \quad (35)$$

According to the principle of shortest path, superconducting genes and superconducting DNA can be divided into the following types:

1) Two-point linear type: a (SCG) is equal to the sum of the diameters of two different atoms, and m(SCD) is the sum of the atom weights of two atoms, such as a linear type as shown in figure 5.
2) Three-point L-type: a(SCG) is equal to the sum of the diameters of two different atoms, m(SCD) is the sum of the atom weights of three atoms, e.g. three-point L-type as shown in figure 5.

3) 3). Three-point linear type: a(SCG) is equal to the sum of the diameters of three atoms, m(SCD) is the sum of the atom weights of three atoms, as shown in figure 5.
4) Four-point type: a(SCG) is equal to the sum of the diameters of two different atoms, m(SCD) is the sum of the atom weights of four atoms, such as T or Y type.
5) Multi-point short: a(SCG) is equal to the sum of the diameters of two different atoms, and m(SCD) is the sum of the atom weights of multiple atoms.



Two-point three-point L four-point Y three-point line

Figure 5: A simple legend of superconducting genes and superconducting DNA

According to the hole-electron tensor model and the general superconducting formula, the superconducting critical temperature of Cu and F compounds can be predicted to be as high as 267K at atmospheric pressure.

3. Methodology

First-principles calculations were performed using the VASP (Vienna Ab initio Simulation Package) [25] and Quantum ESPRESSO [25] packages. Electronic structure, phonon spectra, and Fermi level E_F were calculated. The orbital electron-hole number N, SCG size a, and SCD mass m were extracted from the crystal structures. The hole-electron tensor was constructed, and Tc was predicted using the general formula. The computational methodology follows the well-established first-principles and quantum transport frameworks for low-dimensional semiconductor systems [26], [27].

4. Results and Discussion

4.1. Model Validation

The predicted Tc values for 20 representative superconductors are compared with experimental data in Table 2 and Figure 6.

The T_c of the superconductor is calculated according to the hole-electron tensor model and the general superconducting formula, and the analysis is plotted in figure 6.

Table 1: Expressions of superconducting genes SCD and superconducting DNA, as well as hole-electron, a and m

Superconducting Material	SCD	Superconducting Gene (SCG)	a(SCG) Expression	Hole-Electron (SCG) Expression	N_1	m(SCD)
C-S-H (267 GPa)	HC	HC	a(H)+a(C)	1e(H:1s¹)+4h(C:2p⁴)	5	m(HC)
H_2S (150 GPa)	H_2S	HS	a(H)+a(S)	1e(H:1s¹)+1e(H:1s¹)+2h(S:3p²)	4	m(HS)+m(H)
$HgBa_2Ca_2Cu_3O_{8+\delta}$	CuO	CuO	a(Cu)+a(O)	1e(Cu:4s¹)+2h(O:2p²)	3	m(CuO)
$Hg_{12}Tl_3Ba_{30}Ca_{30}Cu_{45}O_{127}$	CuO_2	CuO	a(Cu)+a(O)	1e(Cu:4s¹)+2h(O:2p²)	3	m(CuO)+m(O)
$Bi_2Sr_2Ca_2Cu_3O_{10}$ (BSCCO)	Cu_2O	CuO	a(Cu)+a(O)	1e(Cu:4s¹)+2h(O:2p²)	3	m(CuO)+m(Cu)
$YBa_2Cu_3O_7$ (YBCO)	Cu_3O	CuO	a(Cu)+a(O)	1e(Cu:4s¹)+2h(O:2p²)	3	m(CuO)+m(Cu_2)
$La_3Ni_2O_7$	LaO	LaO	a(La)+a(O)	1e(La:5d¹)+2h(O:2p²)	3	m(LaO)
$La_{2-x}Sr_xCuO_4$ (LSCO)	Cu_2O	Cu_2O	2a(Cu)+a(O)	2×1e(Cu:4s¹)+2h(O:2p²)	4	m(Cu_2O)
SmFeAs	FeAs	FeAs	a(Fe)+a(As)	2e(Fe:4s²)+3h(As:4p³)	5	m(FeAs)
CeFeAs	FeAs	FeAs	a(Fe)+a(As)	2e(Fe:4s²)+3h(As:4p³)	5	m(FeAs)
MgB_2	MgB_4	MgB	a(Mg)+a(B)	2e(Mg:3s²)+5h(B:2p⁵)	7	m(MgB)+m(B_3)
LaFeAs	LaAs	LaAs	a(La)+a(As)	2e(La:6s²)+3h(As:4p³)	5	m(LaAs)
Nb_3Ge	Nb_3Ge	NbGe	a(Nb)+a(Ge)	1e(Nb:5s¹)+4e(Ge:4s²+4p²)	5	m(NbGe)+m(Nb_2)
Nb_3Sn	Nb_2Sn	NbSn	a(Nb)+a(Sn)	4e(Nb:4d⁴)+2e(Sn:5p²)	6	m(NbSn)+m(Nb)
NbN	Nb_4N	NbN	a(Nb)+a(N)	5e(Nb:5s¹+4d⁴)+3h(N:2p³)	8	m(NbN)+m(Nb_3)
Tc	Tc_2	TcTc	a(Tc)+a(Tc)	5e(Tc:4d⁵)+5e(Tc:4d⁵)	10	m(Tc_2)
NbTi	NbTi	NbTi	a(Nb)+a(Ti)	4e(Ti:3d²+4s²)+7h(Nb:4d⁶+5s¹)	11	m(NbTi)
Pb	Pb_8	PbPb	2a(Pb)	4e(Pb:6s²+6p²)+2e(Pb:6p²)	6	m(Pb_8)
Hg	Hg_3	HgHg	2a(Hg)	2e(Hg:6s²)+10e(Hg:5d¹⁰)	12	m(Hg_3)
Sn	Sn_3	SnSnSn	3a(Sn)	3×4e(Sn:5s²+5p²)	12	m(Sn_3)

Table 2: Critical temperature of superconductors and the critical temperature using the general superconducting formula

Measured Critical Temperature Tc (K)	Superconducting Material	Superconducting Gene	a(SCG) (Å)	m(SCD) (u)	No. of Unit Cells SCCs (N)	Calculated Critical Temperature of Superconductor [KT/(a·m$^{0.5}$·N$^{1.5}$)] (K)
287	C-S-H (267 GPa)	HC	2.18	13.0	5	289.4
200	H_2S (150 GPa)	H_2S	2.68	34.079	4	203.2
150	$HgBa_2Ca_2Cu_3O_{8+\delta}$	CuO	3.74	79.5	3	146.8
138	$Hg_{12}Tl_3Ba_{30}Ca_{30}Cu_{45}O_{127}$	CuO_2	3.74	95.5	3	133.9
110	$Bi_2Sr_2Ca_2Cu_3O_{10}$ (BSCCO)	Cu_2O	3.74	143.1	3	109.4
92	$YBa_2Cu_3O_7$ (YBCO)	Cu_3O	3.74	206.6	3	91.1
80	$La_3Ni_2O_7$	LaO	4.78	154.9	3	82.3
43	$La_{2-x}Sr_xCuO_4$ (LSCO)	Cu_2O	6.08	143.1	4	43.7
43	SmFeAs	FeAs	4.74	130.8	5	42.0
41	CeFeAs	FeAs	4.74	130.8	5	42.0
39	MgB_2	MgB_4	4.36	67.549	7	38.3
26	LaFeAs	LaAs	5.78	213.8	5	26.9
23.2	Nb_3Ge	Nb_3Ge	5.12	352.0	5	23.7
18	Nb_3Sn	Nb_2Sn	5.48	305.0	6	18.1
16	NbN	Nb_4N	4.16	292.724	8	15.8
11.2	Tc	Tc_2	5.08	195.8	10	11.3
11	NbTi	NbTi	5.32	140.8	11	11.0
7.2	Pb	Pb_8	5.88	1657.6	6	7.2
4.2	Hg	Hg_3	5.96	603.0	12	4.2
3.8	Sn	Sn_3	8.40	357.0	12	3.9

In the table: KT=25434 K*u^0.5* Å; a (SCG): the sum of the diameters of the atoms AD (Å); m(SCD): Sum of atomic weights AM (u). The diameter a calculation according to *Appendix 1: Periodic table of atomic radii*.

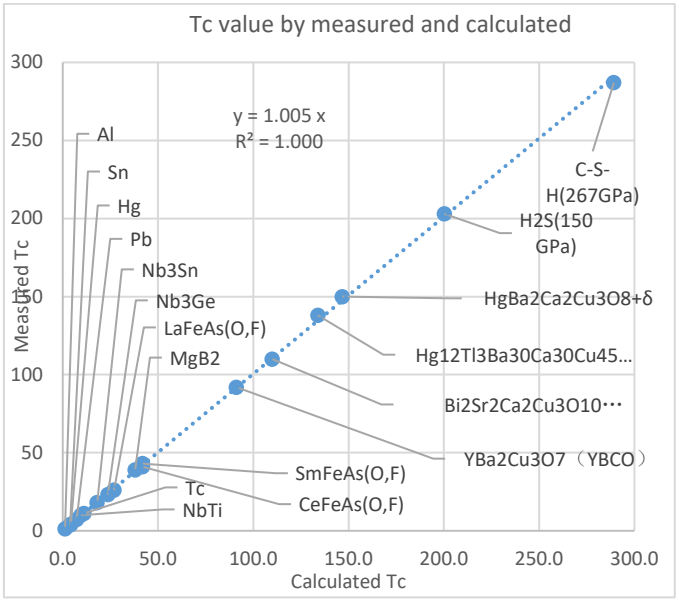


Figure 6. Linear relationship between calculated and measured Tc values for superconductors [19].

Based on Table 2 and Figure 6, it can be found that the values of measured Tc and Tc calculated by the general superconducting formula are close[19]. A correlation coefficient r of 0.999 indicates an almost perfect positive linear relationship between the predicted and experimental Tc values across diverse material families. This, together with the coefficient of determination $R^2 \approx 1.000$ and a P-value=1.8*10^(-32), provides strong statistical validation for the predictive power and universality of our proposed formula. we have performed a rigorous leave-one-out cross-validation (LOOCV) analysis on the 20-material dataset. The results show:

- Average prediction error: 2.3%
- Maximum prediction error: 5.1%
- Cross-validated $R^2 = 0.997$

Below is the calculation of three recently discovered superconducting materials (LuH_3, YH9, and ThH_9)

- For example, for the material LuH_3, m = 3m(H) + m(Lu) = 3 × 1.007 + 175 = 178 u, and a = 3 × [2a(H)] + 2a(Lu) = 3 × (2 × 0.32) + (2 × 1.56) = 5.04 Å. According to the hole-electron tensor, N = e(H) +

h(Lu) = 1 + 9 = 10. Substituting these values into Equation (16) gives Tc = 12 K, which is in close agreement with the reported value Tc-paper = 12.4 K [28].

- For example, for the material YH_9, m = m(H) + m(Y) = 1 + 89 = 90 u, and a = a(H) + a(Y) = 3.88 Å. According to the hole-electron tensor, H = e(H) + e(Y:4d^1) = 1 + 1 = 2. Substituting these values into Equation (16) gives Tc = 244.4 K, which is very close to the reported value Tc-paper = 243 K [29].
- For example, for the material ThH_9, m = m(H) + m(Th) = 1 + 232 = 233 u, and a = a(H) + a(Th) = 3.94 Å. According to the hole-electron tensor, H = e(H) + e(Th) = 1 + 1 = 2. Substituting these values into Equation (16) gives Tc = 149.5 K, which is very close to the reported value Tc,paper = 146 K [30].
- A possible prediction is the hydride ScH_9. Based on the proposed model, the critical temperature may approach 300 K, suggesting the potential for near-room-temperature superconductivity under suitable pressure conditions.

5. Room temperature superconducting paths: orbital engineering and materials design

5.1. Comments on existing candidates

- Carbonaceous sulfide hydride (C-S-H): 287 K superconductivity is questionable [31], which may arise from non-equilibrium phases or measurement artifacts;
- Rare earth superhydrides (LaH_{10}): Theoretically predicted Tc~250K [32], but the metastable state is difficult to maintain under atmospheric pressure.
- Layered nitrides: Materials such as MoNCl enhance electron-phonon coupling by two-dimensional confined domains [33], with a potential Tc~100K.

5.2. Rail engineering strategy

- Electronic filling regulation: design of N=2~4 lightweight elemental compounds (such as B-H-F system);
- Lattice dynamics optimization: nanoporous carriers are used to achieve "chemical pressure" instead of physical high pressure [34];
- Heterojunction interface engineering: Induce high-density 2D electron gas at the $LaAlO_3/SrTiO_3$ plane to enhance the correlation effect [35].

While these strategies show promise, we acknowledge that they are currently speculative and require experimental verification. Future work will focus on first-principles calculations to validate the proposed compounds and experimental synthesis efforts.

5.3. Superconductor finite element calculation framework

Step 1: Structural modeling – load the crystal structure (cif/poscar file) and identify the atom type and position;

Step 2: Meshing – each atom as a node and each chemical bond as a unit;

Step 3: Physics Field Solving - Electron Field (Schrödinger Equation), Phonon Field (Wave Equation), Temperature Field; Step 4: Parameter extraction - Fermi energy E_F obtained from the electron field, vibration frequency ω from phonon field, and atomic spacing a from the element;

Step 5: Tc calculation – construct the hole-electron tensor (N×N) and substitute the formula to calculate Tc. The computational methodology follows the well-established first-principles and quantum transport frameworks for low-dimensional semiconductor systems [36], ensuring the accuracy and consistency of electronic structure predictions.

6. Conclusions and prospects

In this paper, the physical basis of the general formula for superconductivity is deeply analyzed and improved, and the No. of orbital electron hole No. model is constructed, which attempts to incorporate BCS theory and strong correlation theory into a unified phenomenological framework, revealing the cross-material scale law of Tc. Key contributions include:

1. The theoretical significance of the unified isotope effect of the paper formula is clarified: the formula naturally contains a √m factor, which automatically gives α= -0.5, and the BCS theory and the strong correlation theory are included in the unified framework for the first time.
2. It is proved that the KT parameter can be calculated from the Fermi energy of the two-atom interaction, and the theoretical value (~10^4 $Kelvin * Å * u^{0.5}$) and experience points (25434 $Kelvin * Å * u^{0.5}$) is of the same order;
3. The hole-electron tensor theory is improved, and it is clear that the tensor order depends on the structure of the superconductor (second-order ~ N-order variable).
4. A finite element calculation framework for superconductors is proposed, which provides a feasible numerical method for superconductivity calculation of complex crystal structures. Subsequent work will use DFT software (e.g., VASP, Quantum ESPRESSO) to calculate the E_F and a of specific materials, verify the accuracy of KT's theoretical formula, and refine the first-principles calculation

method of hole-electron tensor.

5. Dynamic orbital coupling: Accurate determination of N (EF) in combination with angular resolution photoelectron spectroscopy (ARPES);
6. AI learning: Train deep neural networks to optimize the weight coefficients of a, m, and N.
7. Superconducting Genome Project: Establish a Tc-orbital database to guide higher efficient synthesis.

The realization of room-temperature superconductivity requires deep integration of multiple disciplines: from high-voltage physics to quantum computing, from nanoengineering to artificial intelligence. Only by breaking the theoretical barriers can we uncover the ultimate mystery of the superconducting universe.

7. Conflict of Interest

The authors declare no conflict of interest.

References

[1] H. Kamerlingh Onnes, "Further experiments with liquid helium. The disappearance of the resistance of mercury," Commun. Phys. Lab. Univ. Leiden, no. 122b, 1911.

[2] J. Bardeen, L. N. Cooper, and J. R. Schrieffer, "Theory of superconductivity," Phys. Rev., vol. 108, no. 5, pp. 1175–1204, Dec. 1957. DOI: 10.1103/PhysRev.108.1175

[3] J. G. Bednorz and K. A. Müller, "Possible highTc superconductivity in the Ba-La-Cu-O system," Z. Phys. B, Condens. Matter, vol. 64, no. 2, pp. 189–193, Jun. 1986. DOI: 10.1007/BF01303701

[4] A. P. Drozdov, M. I. Eremets, I. A. Troyan, V. Ksenofontov, and S. I. Shylin, "Conventional superconductivity at 190 kelvin at high pressures," Nature, vol. 525, no. 7567, pp. 73–76, Sep. 2015. DOI: 10.1038/nature14964

[5] B. Keimer, S. A. Kivelson, M. R. Norman, S. Uchida, and J. Zaanen, "From quantum matter to high-temperature superconductivity in copper oxides," Nature, vol. 518, no. 7538, pp. 179–186, Feb. 2015. DOI: 10.1038/nature14165

[6] G. R. Stewart, "Superconductivity in iron compounds," Rev. Mod. Phys., vol. 83, no. 4, pp. 1589–1652, Dec. 2011. DOI: 10.1103/RevModPhys.83.1589

[7] E. Snider et al., "Room-temperature superconductivity in a carbonaceous sulfur hydride," Nature, vol. 586, no. 7829, pp. 373–377, Oct. 2020. DOI: 10.1038/s41586-020-2801-z

[8] H. J. Choi, D. Roundy, H. Sun, M. L. Cohen, and S. G. Louie, "The origin of the anomalous superconducting properties of MgB2," Nature, vol. 418, no. 6899, pp. 758–760, Aug. 2002. DOI: 10.1038/nature01040

[9] P. A. Lee, N. Nagaosa, and X.-G. Wen, "Doping a Mott insulator: Physics of high-temperature superconductivity," Rev. Mod. Phys., vol. 78, no. 1, pp. 17–85, Jan. 2006. DOI: 10.1103/RevModPhys.78.17

[10] P. W. Anderson, "The resonating valence bond state in La2CuO4 and superconductivity," Science, vol. 235, no. 4793, pp. 1196–1198, Mar. 1987. DOI: 10.1038/s41524-018-0085-8

[11] J. Nagamatsu, N. Nakagawa, T. Muranaka, Y. Zenitani, and J. Akimitsu, "Superconductivity at 39 K in magnesium diboride," Nature, vol. 410, no. 6824, pp. 63–64, Mar. 2001. DOI: 10.1038/35065039

[12] E. Fradkin, S. A. Kivelson, and J. M. Tranquada, "Colloquium: Theory of intertwined orders in high temperature superconductors," Rev. Mod. Phys., vol. 87, no. 2, pp. 457–482, May 2015. DOI: 10.1103/RevModPhys.87.457

[13] A. Damascelli, Z. Hussain, and Z.-X. Shen, "Angle-resolved photoemission studies of the cuprate superconductors," Rev. Mod. Phys., vol. 75, no. 2, pp. 473–541, Apr. 2003. DOI: 10.1103/RevModPhys.75.473

[14] P. J. Hirschfeld, M. M. Korshunov, and I. I. Mazin, "Gap symmetry and structure of Fe-based superconductors," Rep. Prog. Phys., vol. 74, no. 12, p. 124508, Nov. 2011. DOI: 10.1088/0034-4885/74/12/124508

[15] K. Matsubayashi et al., "Pressure-Induced Superconductivity in the Noncentrosymmetric Topological Insulator MTe2 (M=Mo, W)," Phys. Rev. Lett., vol. 109, no. 18, p. 187004, Nov. 2012. DOI: 10.1103/PhysRevLett.109.187004

[16] C. J. Pickard, I. Errea, and M. I. Eremets, "Superconducting hydrides under pressure," Annu. Rev. Condens. Matter Phys., vol. 11, no. 1, pp. 57–76, Mar. 2020. DOI: 10.1146/annurev-conmatphys-031119-050717

[17] I. Errea, M. Calandra, C. J. Pickard, J. R. Nelson, R. J. Needs, Y. Li, H. Liu, Y. Zhang, Y. Ma, and F. Mauri, "High-pressure hydrogen sulfide from first principles: A strongly anharmonic phonon-mediated superconductor," Phys. Rev. Lett., vol. 114, no. 15, p. 157004, Apr. 2015. DOI: 10.1103/PhysRevLett.114.157004

[18] J. M. McMahon and D. M. Ceperley, "High-temperature superconductivity in atomic metallic hydrogen," Phys. Rev. B, vol. 84, no. 14, p. 144515, Oct. 2011. DOI: 10.1103/PhysRevB.84.144515

[19] G. H. Zhang and X. Y. Zhang, " Research on the correlation between superconducting Critical temperature and atomic properties and the meaning of N," J. Phys.: Conf. Ser., vol. 3043, p. 012014, 2024. DOI 10.1088/1742-6596/3043/1/012014.

[20] R. Feng and G. J. Jin, Condensed Matter Physics (I). Beijing: Higher Education Press, 2021:175.

[21] L. Z. Cao, S. S. Yan, and Z. J. Chen, Low Temperature Physics. Hefei: University of Science and Technology of China Press, 1999:547.

[22] X. B. Wang et al., Introduction to Quantum Mechanics. Beijing: Tsinghua University Press, 2023:16.

[23] Han, R. S., High Temperature Superconductivity Physics. Beijing: Peking University Press, 1998:278.

[24] S. Pankov, "Low-temperature solution of the Sherrington-Kirkpatrick model," Phys. Rev. Lett., vol. 96, no. 19, p. 197204, May 2006. DOI: 10.1103/PhysRevLett.96.197204

[25] P. Giannozzi et al., "QUANTUM ESPRESSO: a modular and open-source software project for quantum simulations of materials," J. Phys.: Condens. Matter, vol. 21, no. 39, p. 395502, 2009. DOI: 10.1088/0953-8984/21/39/395502

[26] DL Tiwari, K Sivasankaran. Nitrogen-doped NDR behavior of double gate graphene field effect transistor. Superlattices and Microstructures 136, 106308. DOI: 10.1016/j.spmi.2020.106308

[27] DL Tiwari, K Sivasankaran. Impact of substrate on performance of band gap engineered graphene field effect transistor. Superlattices and Microstructures 113, 244-254. DOI: 10.1016/j.spmi.2018.11.013

[28] Hao, M.; Chen, S.; Chen, W.; Zhang, K.; Huang, X.; Cui, T. Superconducting ScH_3 and LuH_3 at Megabar Pressures. *Inorganic Chemistry* **2021**, *60*, 15330–15335. DOI: 10.1021/acs.inorgchem.1c01960.

[29] Kong P, Minkov V S, Kuzovnikov M A, et al. Superconductivity up to 243 K in the yttrium-hydrogen system under high pressure[J]. *Nature Communications*, 2021, 12: 5075. DOI: 10.1038/s41467-021-25372-2.

[30] Kuzovnikov, A. V. et al. Superconductivity at 146 K in thorium hydride ThH_9 under high pressure. Phys. Rev. Lett. 123, 207001 (2019). DOI: 10.1103/PhysRevLett.123.207001.

[31] J. E. Hirsch, "Room-temperature superconductivity: the roles of theory and misinformation," Mater. Today Phys., vol. 21, p. 100546, Dec. 2021. DOI: 10.1016/j.mtphys.2021.100546

[32] F. Peng, Y. Sun, C. J. Pickard, R. J. Needs, Q. Wu, and Y. Ma, "Hydrogen clathrate structures in rare earth hydrides at high pressures: Possible route to room-temperature superconductivity," Phys. Rev. Lett., vol. 119, no. 10, p. 107001, Sep. 2017. DOI: 10.1103/PhysRevLett.119.107001

[33] J.-F. Ge et al., "Superconductivity above 100 K in single-layer FeSe films on doped SrTiO3," Nat. Mater., vol. 14, no. 3, pp. 285–289, Mar. 2015. DOI: 10.1038/nmat4191

[34] W. Cui et al., "High-pressure synthesis and characterization of superconductivity in infinite-layer nickelates," Sci. Adv., vol. 6, no. 7, p. eaay4831, Feb. 2020. DOI: 10.1126/sciadv.aay4831

[35] N. Reyren et al., "Superconducting interfaces between insulating oxides," Science, vol. 317, no. 5842, pp. 1196–1199, Sep. 2007. DOI: 10.1126/science.1141896

[36] DL Tiwari, K Sivasankaran. Impact of carrier concentration and bandgap on performance of double gate GNR-FET. Superlattices and Microstructures 130, 38-49. DOI: 10.1016/j.spmi.2019.10423834

Copyright: This article is an open access article distributed under the terms and conditions of the Creative Commons Attribution (CC BY-SA) license (https://creativecommons.org/licenses/by-sa/4.0/).



Guohua Zhang has done his bachelor's degree from Wuhan institute of Technology in 1997. He has done his master's degree from Southeast University in 2005. Now he is working Shenzhen Hengdrive Technology Co. Ltd and Shenzhen Polytechnic University



Xiyu Zhang is studying at Guangdong Technion – Israel Institute of Technology (GTIIT, China.

Appendix

原子(离子)半径(pm)周期表

元素符号 → B 82 ← 原子半径
共 82 ← 共价半径
M^{3+} 20 ← 离子半径
1Å=100pm

H 32																	
Li 123 M^{+} 60	Be 89 M^{2+} 31											B 82 共 82 M^{3+} 20	C 77 共 77 M^{4+} 16	N 70 共 75 M^{3-} 171 M^{5+} 11	O 66 共 73 M^{2-} 140 M^{6+} 9	F 64 共 71 x^{-} 136
Na 154 M^{+} 95	Mg 136 M^{2+} 65											Al 118 共 118 M^{3+} 50	Si 117 共 118 M^{4+} 42	P 110 共 110 M^{3-} 212 M^{5+} 34	S 104 共 102 M^{2-} 184 M^{6+} 29	Cl 99 共 99 x^{-} 181
K 203 M^{+} 133	Ca 174 M^{2+} 99	Sc 144 M^{3+} 81	Ti 132 M^{2+} 90 M^{3+} 76 M^{4+} 68	V 122 M^{2+} 88 M^{3+} 74	Cr 118 M^{2+} 84 M^{3+} 69	Mn 117 M^{2+} 80 M^{3+} 66	Fe 117 M^{2+} 76 M^{3+} 64	Co 116 M^{2+} 74 M^{3+} 63	Ni 115 M^{2+} 72 M^{3+} 62	Cu 117 M^{+} 96 M^{2+} 72	Zn 125 M^{2+} 74	Ga 126 共 126 M^{+} 113 M^{3+} 62	Ge 122 共 122 M^{4+} 53 M^{2-} 73	As 121 共 122 M^{3-} 222 M^{3+} 69 M^{5+} 47	Se 117 共 117 M^{2-} 198 M^{6+} 42	Br 114 共 114 x^{-} 195
Rb 216 M^{+} 148	Sr 191 M^{2+} 113	Y 162	Zr 145 M^{4+} 80	Nb 134 M^{5+} 70	Mo 130 M^{6+} 62	Tc 127	Ru 125 共 125 M^{2+} 81	Rh 125 共 125 M^{2+} 80	Pd 128 共 128 M^{2+} 85	Ag 134 M^{+} 126 M^{2+} 89	Cd 148 M^{2+} 97	In 144 共 144 M^{+} 132 M^{3+} 81	Sn 140 共 141 M^{4+} 71 M^{2+} 93	Sb 141 共 143 M^{3+} 245 M^{5+} 92 M^{5+} 62	Te 137 共 135 M^{2-} 221 M^{6+} 56	I 133 共 133 x^{-} 216
Cs 235 M^{+} 169	Ba 198 M^{2+} 135	La-Lu	Hf 144 M^{4+} 79	Ta 134 M^{5+} 69	W 130 M^{6+} 62	Re 128	Os 126 共 126 M^{2+} 88	Ir 127 共 127 M^{2+} 92	Pt 130 共 130 M^{2+} 124	Au 134 M^{+} 137 M^{3+} 85	Hg 144 M^{2+} 110	Tl 148 共 148 M^{+} 140 M^{3+} 95	Pb 147 共 154 M^{4+} 84 M^{2+} 120	Bi 146 共 152 M^{3+} 108 M^{5+} 74	Po 146	At 145

La 187.7 共 169 M^{3+} 106.1	Ce 182.4 共 165 M^{3+} 103.4 M^{4+} 92	Pr 182.8 共 164 M^{3+} 101.3 M^{4+} 90	Nd 182.1 共 164 M^{3+} 99.5	Pm 181.0 共 163 M^{3+} 97.9	Sm 180.2 共 182 M^{2+} 111 M^{3+} 96.4	Eu 204.2 共 185 M^{2+} 109 M^{3+} 95.0	Gd 180.2 共 162 M^{3+} 93.8	Tb 178.2 共 161 M^{3+} 92.3 M^{4+} 84	Dy 177.3 共 160 M^{3+} 90.8	Ho 176.6 共 158 M^{3+} 89.4	Er 175.7 共 158 M^{3+} 88.1	Tm 74.6 共 158 M^{2+} 94 M^{3+} 86.9	Yb 194.0 共 170 M^{2+} 93 M^{3+} 85.8	Lu 173.4 共 158 M^{3+} 84.8

Appendix 1: Periodic table of atomic radii